Desalination and Water Treatment
www.deswater.com

doi:10.5004/dwt.2019.24491

165 (2019) 111–123
October

Adsorptive removal of sodium dodecyl sulfate using activated coconut shell based adsorbent: kinetic and thermodynamic study

Pravin S. Bhandari, Parag R. Gogate*

Chemical Engineering Department, Institute of Chemical Technology, Nathalal Parekh Marg, Matunga, Mumbai 400019, India, email: bhandarips74@yahoo.co.in (P.S. Bhandari), pr.gogate@ictmumbai.edu.in (P.R. Gogate)

Received 24 January 2019; Accepted 4 June 2019

ABSTRACT

Adsorptive separation of sodium dodecyl sulfate (SDS) was investigated in the present work using modified adsorbent prepared by thermo-chemical activation of coconut shell based on Phosphoric acid as an activation agent (PAACS-I). The effect of different operating conditions on extent of SDS removal has been studied. Between the investigated pH range of 2.0 to 8.0, the removal of SDS was found to be independent of pH whereas definite variation for all other parameters was established over the investigated range with existence of optimum conditions. Extent of SDS removal as 100%was obtained at natural pH of solution in 120 min under optimized conditions of 80 mg/L as the initial concentration, 2 g/L as the adsorbent loading, 150 rpm as the speed of rotation and 303 K as the operating temperature. The maximum adsorption capacity under optimized condition was determined as 111.1 mg/g. The kinetic data fitted well into the pseudo second order kinetic model. Multi-linear nature of Webber-Morris curve fitting indicated that the intra-Particle diffusion was not the sole controlling mechanism. Isotherm study was performed over the concentration and temperature range as 80–240 mg/L and 303–323 K respectively. Obtained data was analyzed by Langmuir, Freundlich, Temkin and Dubinin-Radushkevich isotherm models and it was clearly demonstrated that the Langmuir model provided better fit indicating monolayer adsorption. Thermodynamic analysis established that adsorption was spontaneous and exothermic. The obtained values of ΔG° and ΔH° from thermodynamic analysis were found to be –36.28 kJ/mol and –9.98 kJ/mol respectively. Desorption of SDS was attempted using ethanol, acidic and alkaline water as the regeneration solvents. Ethanol gave maximum desorption as 95% in 1 h. Overall the work clearly demonstrated the promise of modified adsorbent, PAACS-I for the adsorptive separation of SDS, with good possibility of desorption and reuse.

Keywords: Anionic surfactant; Sodium dodecyl sulfate; Biosorbent; Coconut shell based adsorbent; Thermodynamic study; Isotherm analysis

1. Introduction

Surfactants are among the most common chemicals used in household and industrial applications due to the typical physicochemical characteristics particularly the surface activity. Surfactant molecules are made up of hydrophilic head and hydrophobic tail which imparts them amphiphilic characteristics. Based on chemical structure, surfactants are classified into four types as cationic, anionic, nonionic and zwitter ionic respectively [1]. Anionic surfactants are most commonly used as important ingredients of shampoo, toothpaste, detergents [2], pesticides, personal care products and textile paints [3]. These are also used for enhanced oil recovery, soil remediation, deinking, dispersion, ore flotation, cutting oils and emulsion polymers [2,4]. Due to widespread use and multi-functionality, surfactants are often found in the domestic and industrial wastewater as these may not be completely utilized in the application. Part of surfactant discharged could be degraded naturally. However biodegradation or natural degradation alone is not sufficient when the surfactant is present in large concentration. The residual surfactants especially the anionic ones are responsible for ill effects on aquatic micro-organisms and ecosystem in water

*Corresponding author.

body. The surfactants can also have an impact on the humans if these enter into the food chain. The presence of surfactants can also affect the treatment efficacy of the wastewater treatment plants. For example, effect on sludge dewatering characteristics and enhanced solubility of organic compounds due to the presence of surfactants has been reported [3]. Thus it is important to develop an effective treatment scheme for removal of surfactant which has been attempted in the present work for a specific case of SDS.

SDS is a simple and important anionic surfactant. It is widely used in detergent, shampoos and cosmetics. SDS is considered responsible for symptoms such as depression, labored breath, and diarrhea in animals and also human beings [5]. SDS also gives acute and chronic toxicity in fish. Surfactants increase solubility of organic compounds in water and hence presence of surfactants can lead to enhancement in carcinogenic potential and dermatitis as reported in literature [6]. Considering environmental and health impacts, permissible limits for surfactants is 1 mg/L in water intended for domestic purposes and still low at 0.5 mg/L for potable water [7]. The stringent regulations necessitate the treatment of surfactant containing wastewater and hence the importance of the current work dealing with SDS removal is established.

Various methods such as adsorption [2,8–12], biodegradation [13,14], ultra-filtration [15,16], advanced oxidation [5,17,18] are reported commonly for the treatment of wastewater. Among the methods mentioned above, adsorptive separation of contaminants is widely explored due to ease of fine tuning the adsorbent performance, ability of synthesizing the adsorbent from biomass or waste material and good possibility of large scale operation in continuous mode. Synthesis of adsorbent from various material such as bentonite clay mineral [19], biomass waste like wood, saw dust, sugarcane bagasse, coconut shell, seeds, wood stalk, seed hulls, coffee beans, [20–26], jack fruit peels [27] microalgae [28], etc. have been reported in the literature. In our previous work [29], the adsorptive separation of sodium dodecyl benzene sulfonate (SDBS) using coconut shell based biosorbent has been studied and its effectiveness was demonstrated. The present work reports the application of same biosorbent (PAACS-I) for adsorptive separation for SDS which is another important anionic surfactant. The effect of various operating parameters on the extents of removal of SDS has been studied with detailed kinetics and thermodynamics analysis to provide insights about the adsorption mechanism and heat effects.

2. Materials and methods

2.1. Materials

SDS (99%), ortho-phosphoric acid (85%), glacial acetic acid (99.5%) and toluene (99.9%) were procured from Merck. Sodium bicarbonate (99%) and Acridine orange hemi (Zinc chloride) salt (C.I.46005) (87% dye content) were procured from S.D. Fine Chemicals, India. Deionised water, which was freshly prepared in the laboratory, was used throughout the experimental work. Initially SDS stock solution having 1000 mg/L as the concentration was prepared and the required solutions having different initial concentration for experiments were obtained after appropriate dilution.

2.2. Synthesis of adsorbent

Thermo-chemically activated coconut shell adsorbent based on phosphoric acid activation (PAACS-I) was synthesized using the method described in our earlier work [29]. Coconut shell was crushed using hammer mill and product obtained was sieved to obtain fine powder, which was subsequently dried in hot air oven at 383 K for 3 h. Dried and free flowing powder was subsequently impregnated with 85% ortho-phosphoric acid (the quantity used was in 1:2 ratio). During the impregnation, small aliquots of acid were added followed by intermediate mixing with glass rod so as to ensure proper impregnation. Finally paste like material was obtained, which was kept for 24 h soaking at room temperature and then dried at 383 K for 18 h. Dry impregnated mass obtained was crushed into lower size and calcined at 673 K for 1 h in absence of oxygen. Calcined material was washed with deionised (DI) water to remove excess acid followed by soaking in 1% $NaHCO_3$ solution for 15 h. Supernatant $NaHCO_3$ solution was decanted and remaining material was again washed several times with water till neutral pH of supernatant was obtained. After final wash, slurry was filtered and the obtained cake was dried using hot air at 383 K for a drying time of 14 h. The obtained material was again crushed to reduce size and packed properly for use in the subsequent adsorption experiments.

2.3. Characterization

BET surface area of adsorbent and the pore size distribution have been analyzed based on the Brunauer-Emmett-Teller (BET) method using the ASAP-2020 (Micromeritics, USA) instrument based on multipoint N_2 adsorption-desorption. SEM micrographs of raw coconut shell powder, synthesized and used adsorbent were determined using the Cameca (Model: SU-30,France) Scanning Electron Microscope.

2.4. Experimental procedure

Adsorption experiments were performed in orbital shaking incubator (Model: BTI-4B, Bio-Technics, India) using the synthetically prepared SDS solution. The adsorbent obtained was sieved, before the actual use in adsorption and particles of size range between 100 to 400 μm were used for all experimental trials. Pre-decided quantum of PAACS-I was added into 50 mL SDS solution of known concentration. The shaking speed was adjusted to 150 rpm and maintained constant throughout the work as there should not be any effect of improper mixing. It was also seen visually that all the particles were uniformly suspended during the experiments at this speed of operation. Each trial was performed in duplicate to ensure accuracy of results. After the experiments, laboratory centrifuge (Remi-R8C, India) was used for obtaining a clear solution to be used for analysis. The effect of different parameters such as adsorbent loading(over the range of 0.5–8 g/L), pH of SDS solution (over the range of 2.0–8.0), initial concentration (over the range of 40–160 mg/L) and temperature (over the range of 303 to 323 K) on the extent of adsorption has been investigated. Adsorbent loading of 3 g/L was used for studying effect of pH, which was investigated as first parmeter

and for all remaining trials adsorbent loading of 2 g/L was used, which was found to yield best results. For isotherm study, SDS solution with initial concentration in the range of 80–280 mg/L was used. The quantity of SDS at equilibrium and at any time (based on the withdrawn sample) was estimated using the following equations:

$$q_t = \frac{(C_0 - C_t) \times V}{M} \quad (1)$$

$$q_e = \frac{(C_0 - C_e) \times V}{M} \quad (2)$$

where C_o and C_e are initial and equilibrium concentration of SDS respectively and C_t is periodic concentrations of SDS in the withdrawn samples at any time t in mg/L. q_t and q_e are the adsorption capacity at any time t and at equilibrium in mg/g. V is volume of SDS solution in L and M is mass of adsorbent in g.

2.5. Desorption study

The ease of adsorbate desorption and subsequent reuse of the adsorbent decides the economics of adsorptive separation. In this set of experiments, SDS solution with initial concentration 80 mg/L was used for adsorption trials under optimum conditions. Adsorbent after the trial was filtered out and gently washed to remove unadsorbed SDS. Adsorbent retained on filter medium was further dried at 373 K for 3 h. The dry adsorbent after adsorption trials was used for the desorption study based on different eluent as deionized water, ethanol, acidic (pH 3.5) and alkaline water (pH 11.5) respectively. Desorption trial were carried out for 60 min. Concentration of adsorbate adsorbed at equilibrium (C_{ads}) was obtained as difference between initial (C_0) and equilibrium concentration (C_e) during the adsorption run. Similarly concentration of adsorbate desorbed (C_{des}) was measured using UV-Visible spectrophotometer analysis of the eluent. Extent of desorption was calculated by Eq. (3) as given below.

$$Extent\ of\ Desorption(\%) = \frac{C_{des}}{C_{ads}} \times 100 \quad (3)$$

2.6. Analysis

SDS concentrations in the feed and different withdrawn samples were measured by Acridine orange (ACO) complex method [30]. Typically during the analysis, stock solution was diluted so as to get 10 mL sample of 4 mg/L concentration, recommended for the correct analysis. A similar dilution criterion was used for sample withdrawn periodically. To the sample for analysis, ACO and glacial acetic acid (100 µL each) were added. ACO forms complex with residual surfactant which was further extracted by adding 5 mL of toluene. The obtained mixture was shaken vigorously for 1 min and then added in separating funnel where the phase separation started immediately. Actually 1 min time was sufficient for separation. However for sake of perfect separation, 10 min separation time was followed. The mixture separated into organic and aqueous phases respectively. The lower aqueous layer was discarded and upper organic layer was used for analysis. The concentration of SDS in complex was determined using UV-Visible spectrophotometer (Model: UV-1800, Shimadzu Corporation Analytical and Measuring Instruments Division, Japan) by measuring absorbance at 499 nm.

3. Results and discussion

3.1. Characterization of adsorbents

3.1.1. Scanning electron microscopy (SEM)analysis

SEM images of adsorbent reveals micro details about surface morphology and textural characteristics at high magnification. SEM images of raw coconut shell powder, synthesized PAACS-I and used PAACS-I (after application in adsorption experiments) are shown in Fig. 1. Comparison of SEM micrographs of raw coconut shell (Fig. 1a) and PAACS-I (Fig. 1b) revealed the development of porous structure due to thermo-chemical activation which is important for adsorption. Similar comparison between SEM images of fresh and used adsorbent (Fig. 1c) clearly demonstrated the reduction in porosity due to the SDS adsorption during the usage.

3.1.2. BET surface area and pore size analysis

Thermo-chemical activation of biomass at high temperatures can produce porous structure due to pyrolytic decomposition of lignocellulosic backbone [31]. Coconut shell was chemically treated by phosphoric acid followed by thermal activation at 673 K. The BET surface area and pore size analysis of the obtained adsorbent after activation was done by BET surface area analyzer. The thermo-chemical treatment yielded porous adsorbent with the higher BET surface area as 674 m^2/g and pore volume as 0.395 cm^3/g. Barret-Joyner-Halenda (BJH) adsorption average pore width and desorption pore width were also determined and the obtained values were 20.3 and 30.7Å respectively which confirmed mesoporous nature of adsorbent.

3.2. Effect of pH on the extent of adsorption

pH of solution decides surface charge of adsorbent and hence affects performance of adsorbent due to the variation in adsorbate-adsorbent interactions. To understand the effect of pH, adsorption trials were performed at varying pH. Typical conditions maintained during the study were 80 mg/L as the initial concentration, 303 K as the temperature, 150 rpm as the shaker speed, adsorbent loading (m) as 3 g/L and treatment time as 120 min. Different solutions with varying pH over the range of 2.0 to 8.0 were used. Fig. 2 depicts that 100% SDS removal was obtained at all the pH within the investigated pH range. The point of zero charge of PAACS-I is 3.4 [29], which means below 3.4, the adsorbent surface charge would be negative and above 3.4, surface would be positively charged. Therefore better removal was expected below pH of 3.4. However, the pH of SDS solution did not affect the extent of removal, which can be attributed to the fact that adsorption mech-

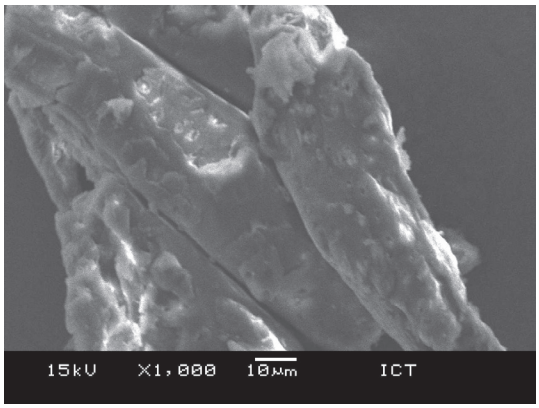

(a)

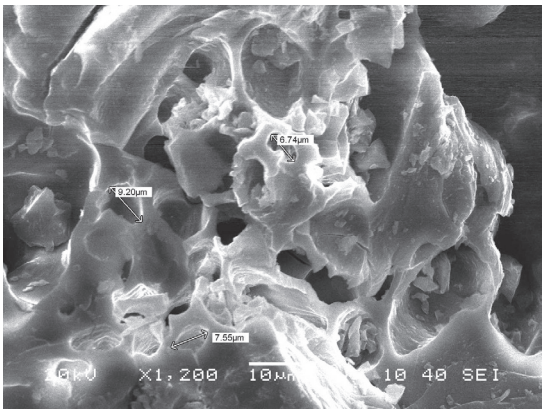

(b)

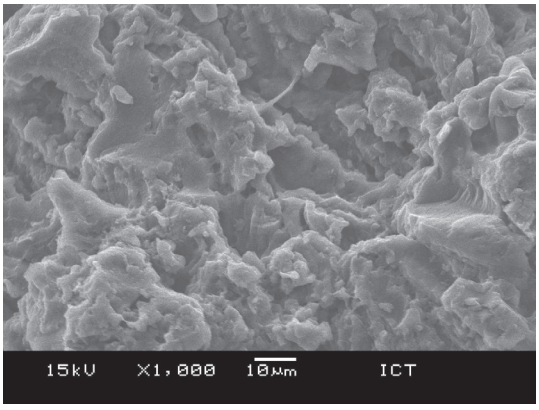

(c)

Fig. 1. SEM micrographs of (a) Raw coconut shell (b) PAACS-I (c) Used PAACS-I.

anism is not controlled dominantly by the electrostatic interactions. The adsorption of surfactant typically occurs by six mechanisms such as ion exchange, ion pairing, hydrogen bonding, adsorption by electron polarization (it is generally observed for adsorbate containing aromatic moiety), adsorption by dispersion forces and hydrophobic bonding [32]. pH dependency is observed mostly in the case of mechanisms based on the electrostatic interactions whereas hydrophobic interactions are always attractive and therefore do not depend on pH of solution. SDS is

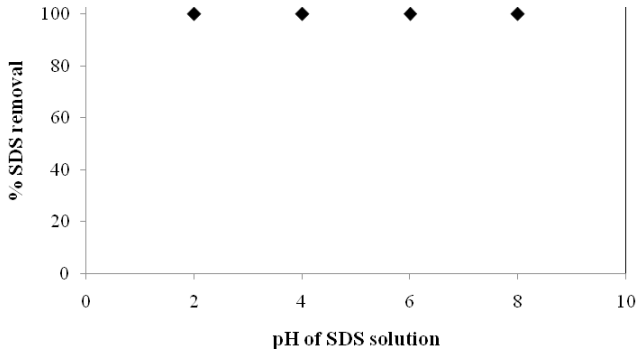

Fig. 2. Effect of pH on extent of SDS removal (C_0: 80 mg/L, m :3 g/L, Temp.: 303 K, Speed: 150 rpm, Time: 120 min).

anionic surfactant, which when dissolved in water ionizes and produces hydrophobic anion. The obtained results suggest that SDS adsorption occurs mostly due to hydrophobic interactions. Role of hydrophobic interactions was also confirmed from desorption study performed in the present work where acidic or alkaline deionised water yielded similar levels of desorption of SDS as discussed in details later. Considering no effect of pH, further trials were performed at natural pH of solution (actual value of 6.87). Similar adsorption behavior based on hydrophobic interactions have also been reported in literature [33–36]. Ihara [36] studied the adsorption of anionic surfactants including SDS on commercial activated carbon (Diahope) and synthetic adsorbent (Amberlite XAD-7). It was reported that the adsorption of anionic surfactants increased with increase in length of alkyl group in surfactant as well as addition of sodium chloride in solution. Both trends confirmed the role of hydrophobic interaction in adsorption of anionic surfactants. Taffarel and Rubio [33] investigated the adsorption of SDBS on CTAB modified zeolite (ZMS) and reported that adsorption of SDBS on ZMS with 100% equivalent cations exchange capacity was independent of pH of solution. Zhao et al. [35] reported that the adsorption of SDBS on carbon black occurs due to stronger hydrophobic interactions in spite of electrostatic repulsion between negatively charged carbon black surface and SDBS anion. Moreno-Castilla [34] also reported role of hydrophobic interactions for effective adsorption of organic compounds on carbon surface.

3.3. Effect of adsorbent loading

The removal using adsorption also depends on the adsorbent loading used in the study. To investigate this effect, trials were conducted for 120 min at 303 K, natural pH and 80 mg/L as the initial concentration. The adsorbent loading was varied between 0.5 to 8 g/L. For a variation of loading from 0.5 to 2 g/L, the SDS removal was observed to increase from 52.1 to 100%, and an increase in loading subsequently to 8 g/L yielded no beneficial results indicating that loading of 2 g/L is the optimum. The obtained trends for the extent of removal at different adsorbent loading have been shown in Fig. 3. Similar results for the effect of loading have been reported by Mane and Babu [38] and Sekar et al. [37] though the observed optimum loading is different. For 100 mg/L aqueous solution of

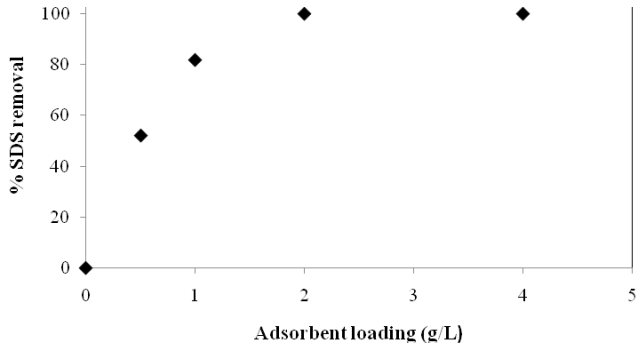

Fig. 3. Effect of adsorbent loading on extent of SDS removal (C_0: 80 mg/L, Temp.: 303 K, Speed: 150 rpm, Time: 120 min).

brilliant green dye and adsorption studies performed at 303 K, the extent of adsorption using NaOH activated saw dust was reported to increase till loading of 4 g/L and thereafter no enhancement in removal was observed up to loading of 30 g/L [38]. For the case of adsorption of Pb(II) using activated carbon prepared from coconut shell, extent of Pb(II) removal was reported to increase to 99% for an increase in loading up to 0.6 g/L. Further increase in loading up to 2 g/L yielded no improvement [37]. Thus it is clearly established that though the trends for effect of adsorbent loading are similar, the actual optimum is different confirming the importance of the current study. Based on the obtained results in the present work, further SDS adsorption trials were conducted using 2 g/L as the optimum adsorbent loading.

3.4. Effect of contact time

Adsorptive separation depends on the time available for adsorbate-adsorbent interaction. Generally the rapid rate of adsorption is observed initially due to higher quantum of vacant sites available [39] and this rate decreases subsequently due to reduced concentration gradient, less vacant sites being available and unfavorable interaction or repulsion between adsorbed molecule and molecules present in solution. Considering these aspects, time profile study is considered essential to decide batch cycle time and evaluate the equilibrium characteristics for adsorption. Obtained variation in the extent of removal and adsorption capacity with time have been depicted in Figs. 4a and b. The trials at optimum conditions of operating parameters were carried out for 300 min. The rapid uptake rate of SDS from solution was observed in first 15 min which progressively decreased and became negligible after 120 min. Around 93, 88, 71 and 58 % SDS removal was obtained in initial 15 min from solutions having initial concentration as 40, 80, 120 and 160 mg/L respectively. The rapid uptake rate in the beginning was attributed to large amount of vacant sites available. With time, vacant sites available decreased thereby reducing the uptake rate. Similar trends were also reported for SDS removal using waste tyre rubber granules [11], and brilliant green dye using NaOH treated saw dust [38]. As the maximum removal (also reaching toward equilibrium) was typically obtained in 120 min in the present work, isotherm trials were performed for a fixed treatment time of 120 min.

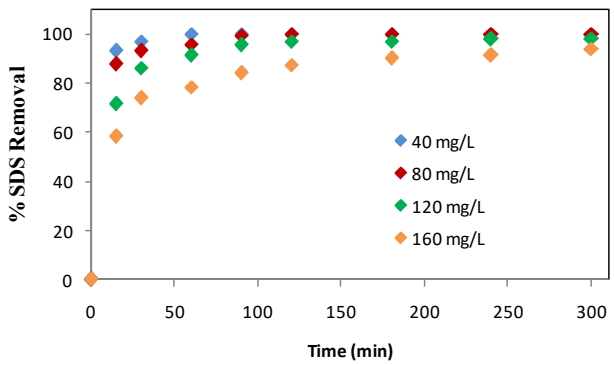

Fig. 4. (a) Effect of concentration and time on extent of SDS removal *m*: 2 g/L, Temp.: 303 K, Speed: 150 rpm, Time: 300 min).

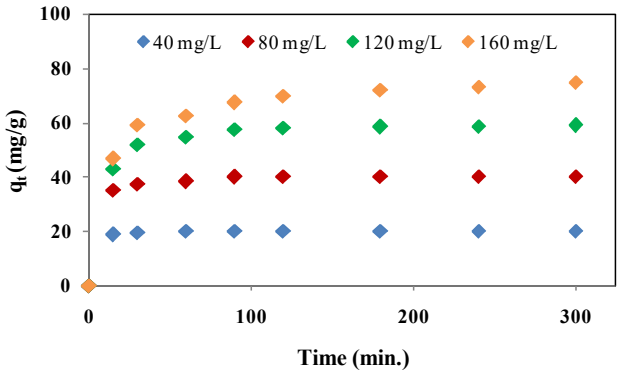

Fig. 4. (b) Effect of concentration and time on adsorption capacity (*m*: 2 g/L, Temp.: 303 K, Speed: 150 rpm, Time: 300 min).

3.5. Effect of initial concentration

Driving force for mass transfer from bulk of adsorbate solution to adsorbent surface depends on the initial concentration of solution. The changes in the initial concentration also affect the extent of removal and adsorption capacity. To investigate the effect, experimental trials were conducted over the range of initial concentration from 40 to 160 mg/L with other conditions maintained constant as agitation speed of 150 rpm, temperature of 303 K and a treatment time of 300 min. The study was combined with investigation into effect of contact time. The obtained trends are shown in Figs. 4a and b. It was observed that with an increase in initial concentration, the adsorption capacity increased whereas extent of removal decreased. Adsorption capacities at equilibrium were obtained as 20, 40, 58.7 and 75 mg/g for different SDS solutions having initial concentration of 40, 80, 120 and 160 mg/L respectively. Enhancement in the SDS adsorbed per unit adsorbent may be attributed to increase probability of collision and increase in driving force for mass transfer [24,40].

Similar trends for the effect of initial concentration are reported in the literature even though reported adsorbent and adsorbate are different, for example the studies with Cu(II) [41] and acid blue dye [42] adsorption. Adsorption capacity of acid activated rubber wood saw dust for Cu(II) was reported to increase from 1.997 to 5.764 mg/g for increase in Cu(II) solution initial concentration from 10 to

40 mg/L. Similarly enhancement in adsorption capacity of NaOH activated fallen leaves of *Ficus racemosa* from 16.92 to 64.94 mg/g for an increase in initial concentration from 50 to 200 mg/L was also reported [42]. It was also reported that extent of dye removal decreased from 99.04% at 50 mg/L dye concentration to 90.36% at 200 mg/L dye concentration, similar to that observed in the current work. It is important to note that even though the trends are same, the extent of increase in adsorption is indeed dependent on the specific adsorbate-adsorbent system making the study reported in the present work important.

3.6. Effect of temperature

Adsorption is energy driven process and hence temperature decides the extent of adsorbate-adsorbent interaction [22,23] and hence the final extent of removal of SDS. To evaluate the effect of temperature, adsorption of SDS on PAACS-I was investigated at different temperatures within the range of 303–323 K and also at varying initial concentrations between 80 to 280 mg/L. It was observed that adsorption capacity decreased with an increase in temperature for all solution concentrations. Fig. 5 represents temperature dependency of SDS adsorption. The reduction in adsorption capacity with temperature is indication of weak adsorption [43,44] as well as exothermic nature of adsorption as also confirmed with thermodynamic studies as discussed later.

3.7. Kinetic study

Kinetic study yields important information about the rate of removal, effect of concentration on extent of removal, time required to achieve equilibrium and mechanism of adsorption. Kinetic data provides insight about the dynamic behavior of adsorption system [28] and information obtained can be used for design of commercial scale adsorption process. Generally adsorption occurs in three steps limited by the bulk diffusion, film diffusion and pore diffusion. Slowest step among three is considered as rate controlling step which governs the rate and performance of adsorption process at commercial scale [45]. The obtained data was correlated with various kinetic models and kinetic data fitting was done with an objective of obtaining the design parameters.

3.7.1. Pseudo first order model

Lagergren's kinetic equation popularly known as pseudo first order equation was used in the current work for data fitting. The mathematical form of the model [47] is given by Eq. (4) as follows:

$$\ln\left(q_e - q_t\right) = \ln q_e - k_1 t \tag{4}$$

where q_e (mg/g) is adsorption capacity at equilibrium, q_t (mg/g) represents adsorption capacity at any time t (min) and k_1 is pseudo first order rate constant (min^{-1}). Fig. 6 represents the obtained kinetic plot for the pseudo first order model whereas the obtained values of k_1 and q_e are mentioned in Table 1. The average value of regression coefficient (R^2) was calculated as 0.898. The equation obtained from data fitting was used to evaluate the values of $q_{e(cal)}$. The experimental values of q_e denoted as $q_{e(exp)}$ were 20, 40, 58.8 and 75 mg/g for initial concentrations as 40, 80, 120 and 160 mg/L respectively. The values of q_e calculated by obtained pseudo first order after data fitting denoted as $q_{e(cal)}$ for similar concentration were 15.94, 19.34, 20.12 and 34.22 mg/g respectively. Significant difference between $q_{e(exp)}$ and $q_{e(cal)}$ and less value of R^2 indicated that pseudo first order kinetic model does not fit the experimental data.

3.7.2. Pseudo second order model

The linearized form of the Pseudo second order model [48] is expressed by Eq. (5) given below.

$$\frac{t}{q_t} = \frac{1}{k_2 q_e^2} + \frac{1}{q_e} t \tag{5}$$

where k_2 is pseudo second order rate constant (g/mg min). The plot of t/q_t versus t was used to obtain values of k_2 and subsequently, $q_{e(cal)}$. Fig. 7 represents pseudo second order kinetic plot whereas the obtained values of kinetic parameters are shown in Table 1. The values of $q_{e(cal)}$ obtained from pseudo second order plot were 20.41, 41.67, 62.50 and 76.92 mg/g respectively, which were quite close to the obtained

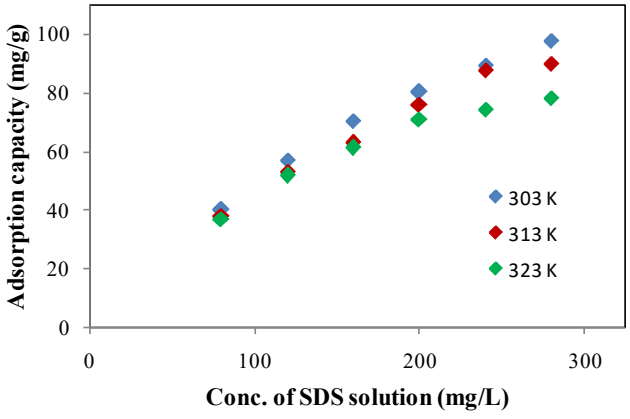

Fig. 5. Effect of temperature (C_0: 80–280 mg/L, m: 2 g/L, Speed: 150 rpm, Time: 120 min).

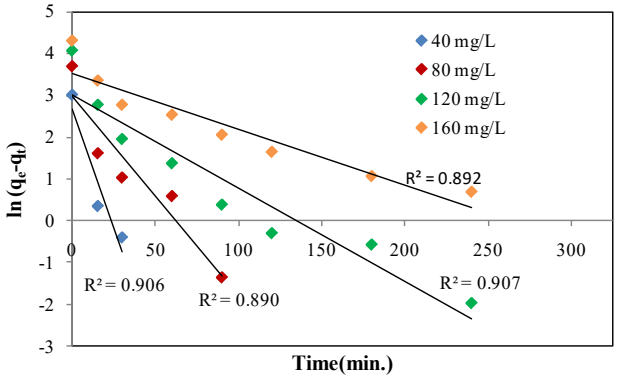

Fig. 6. Pseudo first order kinetic plot (C_0: 40–160 mg/L, m: 2 g/L, Temp.: 303 K, Speed: 150 rpm, Time: 300 min).

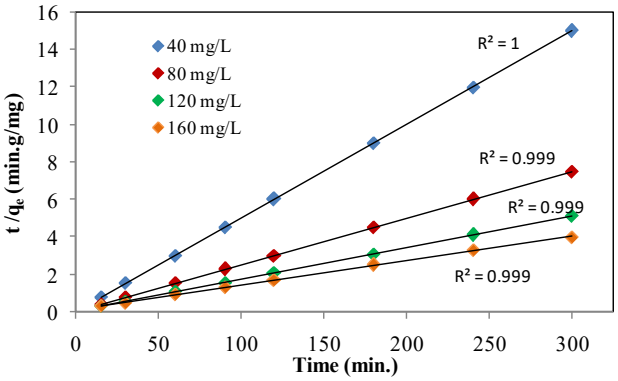

Fig. 7. Pseudo second order kinetic plot (C_0: 40–160 mg/L, m: 2 g/L, Temp.: 303 K, Speed: 150 rpm, Time: 300 min).

experimental values, as compared to the psuedo first order model predictions. The average value of R^2 was found to be 0.9992. The obtained value of R^2 for fitting, confirmed better matching of experimental and calculated values of q_e from the model establishing that pseudo second order equations provide best fit among the different investigated kinetic models. From the obtained values of kinetic model constants as presented in Table 1, it can be said that k_2 decreased from 0.073 to 0.001 g/mg min for a change in concentration from 40 to 160 mg/L respectively. The results are attributed to increased competition between SDS molecules for adsorption with an increase in concentration as finite active sites were available.

3.7.3. Error analysis

Two error functions, the average relative error (*ARE*) and the sum of absolute errors (*EABS*) [49] were used to validate the kinetic models in addition to correlation coefficient R^2. The experimental value q_e designated as $q_{e(exp)}$ and obtained value of $q_{e(cal)}$ from pseudo first order and second order kinetic model were used to calculate the values of ARE and EABS for range of concentration between 40 to 160 mg/L at optimum operating conditions.

3.7.3.1. The average relative error (ARE) function

ARE function quantifies the error distribution across the range of concentration studied and can be calculated using the Eq. (6) as follows.

$$ARE = \frac{100}{n}\sum_{i=1}^{n}\left|\frac{q_{e(cal)} - q_{e(\exp)}}{q_{e(\exp)}}\right| \quad (6)$$

where n represents the number of data points, $q_{e(cal)}$ and $q_{e(exp)}$ are the calculated and experimental values of equilibrium adsorption capacity (mg/g).

Table 1
Kinetic parameters (C_0: 40–160 mg/L, m: 2 g/L, Temp.: 303 K, Speed: 150 rpm, Time: 300 min)

Kinetic model	Parameter	Values			
Pseudo first order	C_0 (mg/L)	40	80	120	160
	$q_{e(exp)}$ (mg/g)	20	40	58.8	75
	$q_{e(cal)}$ (mg/g)	15.94	19.34	20.12	34.22
	K_1 (min^{-1})	0.113	0.047	0.022	0.013
	R^2	0.906	0.890	0.907	0.892
	ARE	3	5.722	7.294	5.95
	EABS	5.4	20.6	38.6	40.1
Pseudo second order	C_0 (mg/L)	40	80	120	160
	$q_{e(exp)}$ (mg/g)	20	40	58.8	75
	$q_{e(cal)}$ (mg/g)	20.41	41.67	62.50	76.92
	K_2 (g/mg·min)	0.073	0.011	0.003	0.001
	R^2	1	0.999	0.999	0.999
	ARE	0.2267	0.463	0.6991	0.2849
	EABS	0.4081	1.666	1.923	7.698
Intra-particle diffusion	C_0 (mg/L)	40	80	120	160
First stage	K_{1d} (mg/g·$min^{-0.5}$)	4.8	9.056	9.747	11.01
	C_1 (mg/g)	–	–	1.151	0.872
	R_1^2	1	1	0.984	0.992
Second stage	K_{2d} (mg/g·$min^{-0.5}$)	0.358	0.68	1.186	2.018
	C_2 (mg/g)	17.26	32.41	45.57	47.69
	R_2^2	0.982	0.957	0.976	0.989
Third stage	K_{3d} (mg/g·$min^{-0.5}$)	–	0.023	0.123	0.764
	C_3 (mg/g)	–	39.63	56.63	61.54
	R_3^2	–	0.451	0.955	0.981

3.7.3.2. The sum of absolute error function (EABS)

EABS is calculated as per the following equation:

$$EABS = \sum_{i=1}^{n} \left| q_{e(cal)} - q_{e(\exp)} \right| \quad (7)$$

The obtained values of *ARE* and *EABS* for kinetic trials are mentioned in Table 1. It can be seen that the values of error function *ARE* and *EABS* are smaller for pseudo second order equation compared to pseudo first order equation. From the comparison of values of R^2 and values of error function *ARE* and *EABS*, it is established that pseudo second order kinetic model fits data better compared to pseudo first order model.

3.7.4. Intra-particle diffusion model

Pseudo first order and second order equation does not clearly identify the prevailing diffusion mechanisms [50]. Intra-particle diffusion model proposed by Weber and Morris provides an insight about the possible controlling diffusion mechanisms and the resistances due to intra-particle and external film diffusions [51]. Eq. (8) represents the mathematical form of Weber-Morris equation

$$q_t = k_{id} t^{1/2} + C \quad (8)$$

where q_t is amount of solute adsorbed per unit mass of adsorbent (mg/g) at any time t, k_{id} represents intra-particle diffusion constant (mg/g $min^{0.5}$) and constant C represents the thickness of boundary layer. The increase in value of C indicate greater contribution of boundary layer effect on adsorption [43]. Typically if the straight line plots of q_t with $t^{1/2}$ pass through the origin, intra-particle diffusion is sole controlling mechanism. Deviation from linearity indicate that other diffusion mechanism also controls the extent of adsorption [52–54]. Fig. 8 shows Weber-Morris plot obtained in the present work based on the Eq. (8) and the values of intra-particle diffusion rate constant k_{id} and intercept C obtained for various concentrations are shown in Table 1. It can be clearly seen that entire graph is non-linear with different zones where straight line fitting with different slopes is possible indicating that intra-particle diffusion is not the sole controlling mechanism. Steep first portion (not shown in Fig. 8 for sake of clarity) represents rapid adsorption on external surface. The rapid adsorption rate in the beginning is attributed to relatively faster external diffusion from bulk to surface of adsorbent [55], unoccupied surface area and large number of vacant sites [56]. Second portion represents gradual adsorption where intra-particle diffusion is rate controlling and in the last stage, adsorption slows down finally reaching the equilibrium [57]. It is important to note that the plot for higher initial concentrations exhibited three distinct stages whereas at the lowest initial concentration of 40 mg/L, only two stages were observed. For for trial using 40 mg/L, the obtained values of k_{id} for first stage and second stage are 4.8 and 0.358 mg/ g $min^{0.5}$ respectively. The values of k_{id} for all other initial concentrations for all the three stages have been depicted in Table 1. It was observed that for all the concentrations, the value of k_{id} progressively decreased from stage 1 to stage 3. Also the values of k_{id} for first stage increased with initial concentration. For typical values of 40, 80, 120 and 160 mg/L as the initial concentrations, values of k_{id} for first stage are 4.8, 9.056, 9.747 and 11.01 mg/g $min^{0.5}$ respectively. The enhancement is obtained due to increase in driving force at higher concentrations [58]. Similar trends in terms of increase with concentration are observed for intercept C which represents the thickness of boundary layer. The greater value of C represents more role of boundary layer in mass transfer control [52].

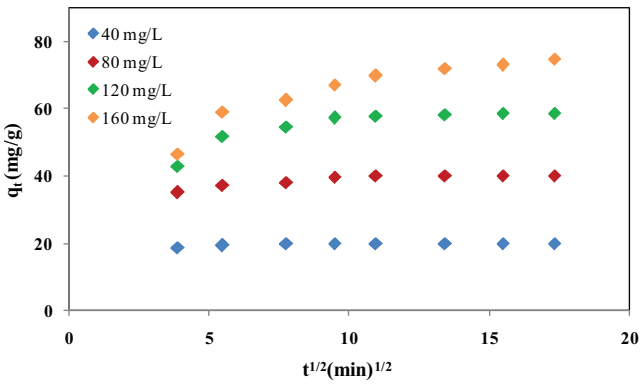

Fig. 8. Weber Morris plot (C_0: 40–160 mg/L, m: 2 g/L, Temp.: 303 K, Speed: 150 rpm, Time: 300 min).

3.8. Adsorption equilibrium studies

Adsorption equilibrium analysis establishes relationship between pollutant concentration remaining in solution at the equilibrium and that adsorbed per unit mass of adsorbent at constant temperature [59]. It also provides information about the adsorbate interaction with adsorbent [60], maximum adsorption capacity and distribution of adsorbate over the surface [54]. To understand these issues isotherm trials were performed at different temperatures over the range of 303–323 K at optimum operating conditions and varying SDS solution concentration over the range 80–280 mg/L and the obtained data was correlated with Langmuir, Freundlich and Temkin adsorption isotherm models.

3.8.1. Langmuir isotherm model

Adsorption isotherm proposed by Langmuir [61] assumes monolayer adsorption with no interaction between the adsorbate molecules. The linearized form of the model is represented as follows:

$$\frac{C_e}{q_e} = \frac{1}{q_m} C_e + \frac{1}{q_m K_L} \quad (9)$$

The values of the model parameters, q_m and K_L were evaluated from slope ($1/q_m$) and intercept ($1/(q_m K_L)$) obtained for the linear fitting of plot of C_e/q_e against C_e. Fig. 9 depicts the obtained plot of Langmuir isotherm model. The obtained model parameters from plot have been represented in Table 2. With an increase in temperature from 303 to 323 K, the value of K_L and q_m decreased progressively from 0.11 to 0.09 L/g and 111.1 to 90.9 mg/g respectively. Both trends confirm the exothermic nature of SDS adsorption on PAACS-I. It was also observed that

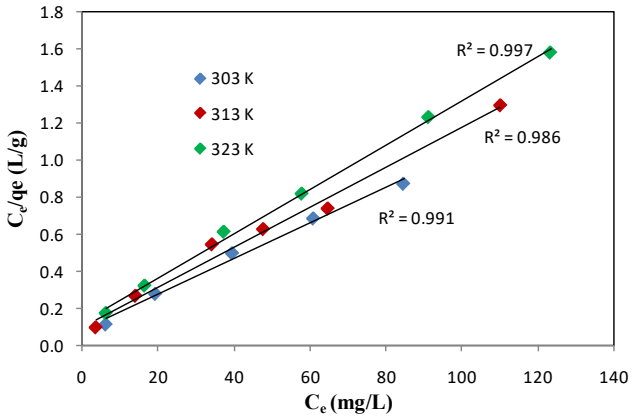

Fig. 9. Langmuir isotherm plot (C_0: 80–280 mg/L, m: 2 g/L, Temp.: 303–323 K, Speed: 150 rpm, Time: 120 min).

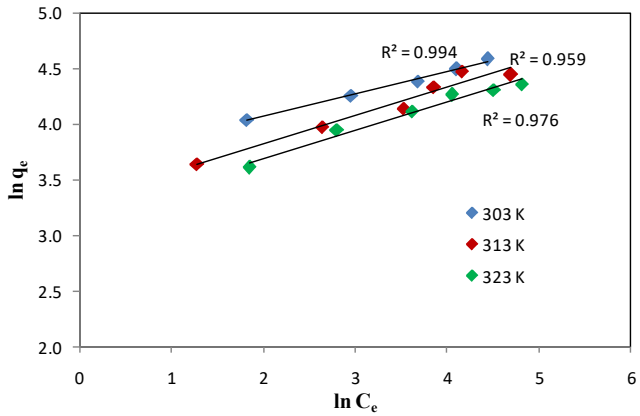

Fig. 10. Freundlich isotherm plot (C_0: 80–280 mg/L, m: 2 g/L, Temp.: 303–323 K, Speed: 150 rpm, Time: 120 min).

Table 2
Isotherm parameters (C_0: 80–280 mg/L, Temp: 303–323 K, m: 2 g/L, Speed: 150 rpm, Time: 120 min)

Isotherm model	Parameters	Values		
		303 K	313 K	323 K
Langmuir	q_m(mg/g)	111.1	100.0	90.9
	K_L(L/mg)	0.11	0.10	0.09
	R^2	0.991	0.986	0.997
Freundlich	K_F (mg/g)(L/mg)$^{1/n}$	38.78	27.39	24.26
	n	4.92	3.94	3.97
	R^2	0.994	0.959	0.976
Temkin	B_T(mg/g)	15.18	15.15	14.04
	K_T(L/mg)	6.00	2.91	2.28
	R^2	0.976	0.925	0.992
Dubinin-Radushkevich	q_s *(mg/g)*	86.3	71.5	68.7
	E(KJ/mol)	0.408	0.5	0.353
	R^2	0.72	0.734	0.838

SDS equilibrium adsorption capacity increased with an increase in concentration due to higher driving force available at higher loadings [39].

3.8.2. Freundlich isotherm model

Freundlich adsorption isotherm [62] represents an empirical model for adsorption on heterogeneous surface differing in affinity for adsorbate. Eq. (10) represents linear form of Freundlich isotherm.

$$\ln q_e = \ln K_F + \frac{1}{n}\ln C_e \tag{10}$$

The value of Freundlich model constant n indicates adsorption affinity and favorability of adsorption process whereas K_F represents biosorption capacity. The values of isotherm constants were obtained from the isotherm plot depicted in Fig. 10. Adsorption process is favorable for values of n between 2–10, moderately difficult for n between 1–2 and poor for n less than 1 [63]. Values of isotherm parameters are shown in Table 2. The obtained values of n in the present work were 4.92, 3.94 and 3.97 respectively confirming that adsorption of SDS is favorable. Biosorption capacity represented by K_F was observed to decrease from 38.78 to 24.26 (mg/g)(L/mg)$^{1/n}$ with an increase in temperature from 303 K to 323 K. This further confirmed that the adsorption is exothermic.

3.8.3. Temkin isotherm model

Temkin and Pyzev [64] proposed isotherm model based on adsorbate-adsorbent interaction, for which the linearized form [52] is represented as:

$$q_e = B_T \ln K_T + B_T \ln C_e \tag{11}$$

where K_T(L/mg) and B_T(mg/g) are Temkin model constant. The obtained values of Temkin's model constant from Fig. 11 are shown in Table 2. For temperature change from 303 to 323 K, B_T was observed to decrease from 15.18 to 14.04 mg/g whereas K_T decreased from 6 to 2.28 L/mg. Both trends indicate that the adsorption is exothermic in nature, consistent with earlier isotherm predictions.

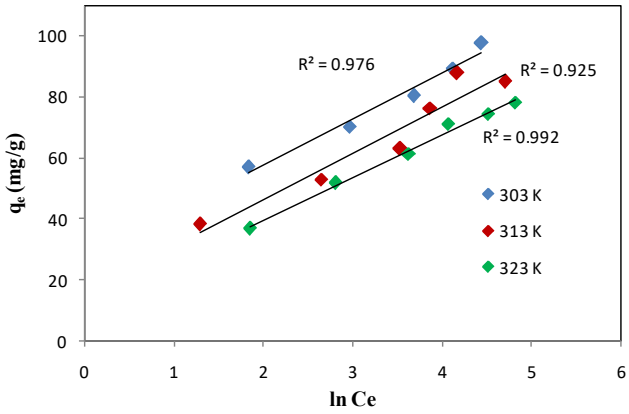

Fig. 11. Temkin isotherm plot (C_0: 80–280 mg/L, m: 2 g/L, Temp.: 303–323 K, Speed: 150 rpm, Time: 120 min).

3.8.4. Dubinin-Radushkevich isotherm model

Isotherm model proposed by Dubinin-Radushkevich (DR) is generally applied to describe the adsorption mechanism with Gaussian energy distribution on heterogeneous surface [60,65]. It is mainly used to distinguish between physical and chemical adsorption. The mathematical form of the model is expressed as:

$$q_e = q_s \exp(-B_{DR}\left(\varepsilon^2\right) \quad (12)$$

where q_e represents equilibrium adsorption capacity (mg/g), q_s is theoretical isotherm saturation capacity (mg/g), B_{DR} is DR isotherm constant related to mean free energy of adsorption (mol²/J²) and ε is Polanyi potential related to biosorption energy [28] expressed by the following equation:

$$\varepsilon^2 = RTln\left[1+\frac{1}{C_e}\right] \quad (13)$$

where R is ideal gas constant (J/mol K) and T is operating temperature (K). It can be understood from Eq. (13) that Polanyi potential is temperature dependent term.

Plot of linearized form of DR isotherm model equation represented below was used to determine values of isotherm parameters.

$$\ln q_e = \ln q_s - B_{DR}\varepsilon^2 \quad (14)$$

Values of q_s and B_{DR} were determined from slope and intercept obtained from plot demonstrated in Fig. 12. The mean free energy of adsorption (E) required for transferring adsorbate from infinity in the solution (hypothetically considered) to solid surface was determined subsequently by following equation:

$$E = \frac{1}{\sqrt{2B_{DR}}} \quad (15)$$

The obtained values of q_s, E and R^2 for the model fitting are shown in Table 2.

Mean biosorption energy E provides important information about governing mechanism in terms of the physical or chemical nature of adsorption. For value of E < 8 kJ/mol, physisorption controls adsorption process. If E > 16 kJ/mol, chemisorption controls adsorption process and ion exchange dominates for 8 < E <16 kJ/mol [43]. The obtained value of E were much less than 8 kJ/mol which confirmed that adsorption occurred by physisorption.

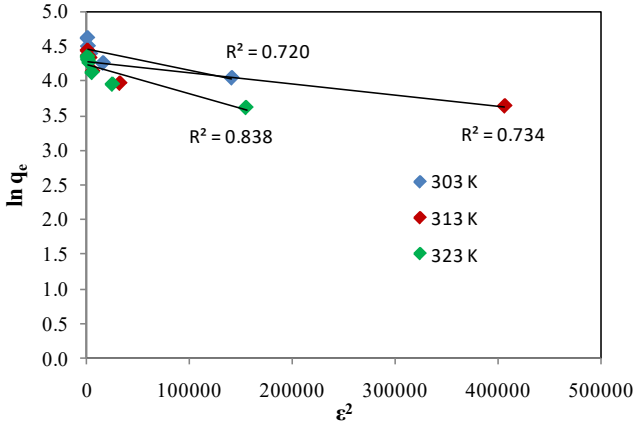

Fig. 12. Dubinin-Radushkevich isotherm plot (C_0: 80–280 mg/L, m: 2 g/L, Temp.: 303–323 K , Speed: 150 rpm, Time: 120 min).

Comparing of the average value of R², Langmuir isotherm provided better fit compared to all the other isotherm models. The values of R² obtained from Langmuir, Freundlich, Temkin and Dubinin-Rudeshkevich isotherm were 0.993, 0.976, 0.964 and 0.764 respectively. Similar trends were also reported in the literature for adsorption of SDS using activated carbon prepared from sustainable feedstock [66]. Comparison of the adsorption capacities of various reported adsorbent for SDS adsorption with that obtained for the current work is shown in Table 3. It can be clearly seen from the reported data that the adsorbent applied in the current work offers excellent promise for removal of SDS.

3.9. Thermodynamic analysis

The values of enthalpy change ($\Delta H°$), free energy change ($\Delta G°$) and entropy change ($\Delta S°$) during adsorption of SDS were calculated using Van't Hoffs equation represented below:

$$lnK = -\frac{\Delta G^\circ}{RT} = -\frac{\Delta H^\circ}{R}\left(\frac{1}{T}\right) + \frac{\Delta S^\circ}{R} \quad (16)$$

where K is dimensionless equilibrium constant obtained by multiplying Langmuir isotherm constant expressed in L/mol with molar density of water (55.5 mol/L) [67]. Fig. 13 depicts the obtained plot of ln(K) versus $1/T$ whereas the obtained values of thermodynamic parameters are given in Table 4. The negative value of free energy and enthalpy change established that adsorption of SDS is spontaneous and exothermic [54]. The obtained value of $\Delta H°$ (–9.98 kJ/mol) was observed to be less than 40 kJ/mol suggesting physical nature of adsorption [54]. The obtained positive value of $\Delta S°$ established the excellent affinity of acid activated coconut shell based biosorbent for SDS and increase in the randomness as also reported in the literature [68]. The positive value of$\Delta S°$ is also an indication of hydrophobic bonding [69].

3.10. Desorption study of equilibrated adsorbent for analyzing reuse

The ease and extent of desorption are important considerations in adsorptive separation methods as this decides the reusability of the adsorbent. The desorption studies also provides an important insight about the mechanism of adsorption. If desorption occurs by acidic or alkaline water then adsorption mechanism is based on ion exchange whereas desorption by deionised water is an indication of weak adsorption [70]. As established in our previous work, the point of zero charge of adsorbent used was 3.4 [29]. The extent of SDS adsorption was not affected over the range of 2.0–8.0 which is an indication that ion exchange is not

Table 3
Comparison of adsorbent reported for SDS adsorption

Adsorbent used	% Removal	q_m (mg/g)	Ref.
PAACS-I	100	111.1	Present work
Chitosan hydrogel beads	99	76.9	[7]
Aquaguard waste activated carbon	98	61.46	[66]
Granular activated charcoal	96	3.750	[72]
Waste tyre rubber granules	96.5	4.164	
Wood charcoal	88	5.170	
Silica gel	92	5.181	
Pine cone bio mass	39.53	95.75	[73]
Standard activated carbon	81	178.6	[74]
NH_4Cl induced pomegranate wood waste	99	117.2	

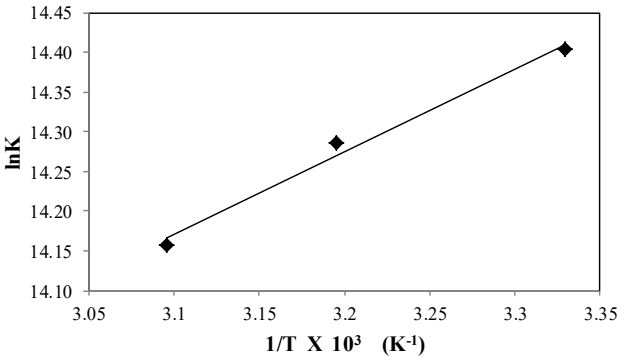

Fig. 13. Van't Hoffs plot for adsorption of SDS on PAACS-I (C_0: 80 –280 mg/L, m: 2 g/L, Speed: 150 rpm, Time: 120 min).

Table 4
Thermodynamic parameters (C_0: 80–280 mg/L, Temp.: 303–323 K, m: 2 g/L, , Speed: 150 rpm, Time: 120 min)

ΔG° (KJ/mol)			ΔH°	ΔS°
303 K	313 K	323 K	(KJ/mol)	(KJ/mol)
–36.28	–35.988	–35.66	–9.98	0.0866

responsible for adsorption. All desorption trials were carried out for 60 min. Desorption trials with acidic and alkaline water at 3.0 and 11.5 pH yielded only 6 and 10.6 % desorption of SDS confirming that pH change does not facilitate desorption. Desorption trials with DI water yielded only 28% desorption of SDS. Similar results were also reported for desorption of SDS from chitosan in the presence of crystal violet dye. No desorption of SDS from chitosan with alkaline water was observed over the pH range of 11.0–14.0 [7]. The observed results with desorption also confirmed that adsorption is dominated by the hydrophobic interactions. The use of solvents like organic solvents like ethanol for desorption of material adsorbed with hydrophobic interactions is reported in literature [71]. Therefore desorption experiments were conducted with ethanol. 95% as the extent of desorption of SDS was obtained using ethanol in 60 min. 100% adsorption of SDS by PAACS-I and maximum desorption obtained using ethanol indicates that adsorptive separation of SDS using PAACS-I is promising method.

4. Conclusions

Effective adsorptive separation of SDS by phosphoric acid activated coconut shell based adsorbent has been demonstrated in the work with complete removal of SDS obtained under the optimized conditions. Removal of SDS at various solution pH was found to be similar which indicated that adsorption occurs mainly by hydrophobic interaction. Adsorption capacity decreased with increase in adsorption loading and increased with the initial concentration of SDS solution. Kinetic data fitting and error analysis revealed that pseudo second order model provides best fit. Data analysis also done by Weber-Morris model indicated that the intra-particle diffusion is not the sole controlling mechanism. Langmuir, Freundlich, Temkin and DR isotherm models were used to analyze the isotherm data. It was observed that Langmuir isotherm provided best fit indicating monolayer adsorption and homogeneous nature of adsorption sites. Thermodynamic analysis of isotherm data revealed SDS adsorption on PAACS-I is exothermic and spontaneous. Desorption of SDS from adsorbent investigated using acidic and alkaline water, deionized water and ethanol confirmed that acidic and alkaline water as well as deionized water gave poor desorption whereas maximum desorption was obtained using ethanol. Based on complete removal of SDS, pH independent adsorption and possibility of regeneration of adsorbent as well as spontaneous nature of adsorption, PAACS-I has been clearly demonstrated as a promising adsorbent for removal of SDS from effluent.

Symbols

PAACS-I — Phosphoric acid activated coconut shell activated carbon
C_0 — Initial SDS concentration (mg/L)
C_t — SDS concentration (mg/L) at any time t
C_e — Final SDS concentration (mg/L)
C_{des} — Concentration of adsorbate desorbed (mg/L)
C_{des} — Concentration of adsorbate adsorbed at equilibrium (mg/L)
V — Volume of SDS solution (L)
M — Mass of adsorbent added (g)
m — Adsorbent loading (g/L)
q_t — Adsorption capacity at any time t (mg/g)
q_e — Adsorption capacity at equilibrium (mg/g)
$q_{e(cal)}$ — Calculated adsorption capacity at equilibrium (mg/g)
q_m — Maximum adsorption capacity (mg/g)
t — Time (min)
k_1 — Pseudo first order rate constant (1/min)
k_2 — Pseudo second order rate constant (g/mg min)
b — Langmuir isotherm constant (L/mg)

K_F — Freundlich isotherm constant indicating biosorption capacity ((mg/g)(L/mg)$^{1/n}$)
n — Freundlich isotherm constant representing Adsorption affinity
K_T — Temkin model constant (L/mg)
B_T — Temkin model constant (mg/g)
— Theoretical saturation capacity of adsorbent (mg/g)
B_{DR} — Dubinin-Radushkevich isotherm constant (mol^2/J^2)
ε — Polanyi potential
E — Mean free energy of adsorption (J/mol)
$\Delta G°$ — Free energy change (KJ/mol)
$\Delta S°$ — Entropy change (KJ/mol K)
$\Delta H°$ — Enthalpy change during adsorption (KJ/mol)
K — Dimensionless equilibrium constant
R — Ideal gas constant (KJ/mol K)
T — Temperature (K)
ARE — Average relative error
EABS — Absolute error

References

[1] K. Majewska-Nowak, I. Kowalska, M. Kabsch-Korbutowicz, Ultrafiltration of SDS solutions using polymeric membranes, Desalination, 184 (2005) 415–422.
[2] P. Li, M. Ishiguro, Adsorption of anionic surfactant (sodium dodecyl sulfate) on silica, Soil Sci. Plant Nutr., 62 (2016) 223–229.
[3] F. Ríos, M. Olak-Kucharczyk, M. Gmurek, S. Ledakowicz, Removal efficiency of anionic surfactants from water during UVC photolysis and advanced oxidation process in H_2O_2/UVC system, Arch. Environ. Prot., 43 (2017) 20–26.
[4] C.E. Hoeft, R.L. Zollars, Adsorption of single anionic surfactants on hydrophobic surfaces, J. Colloid Interface Sci., 177 (1996) 171–178.
[5] H.M. Nguyen, C.M. Phan, T. Sen, Degradation of sodium dodecyl sulfate by photoelectrochemical and electrochemical processes, Chem. Eng. J., 287 (2016) 633–639.
[6] P. Das Purakayastha, A. Pal, M. Bandopadhyay, Adsorption of anionic surfactant by a low-cost adsorbent, J. Environ. Sci. Health. A. Tox. Hazard. Subst. Environ. Eng., 37 (2002) 925–938.
[7] A. Pal, S. Pan, S. Saha, Synergistically improved adsorption of anionic surfactant and crystal violet on chitosan hydrogel beads, Chem. Eng. J., 217 (2013) 426–434.
[8] A. Ariapad, M.A. Zanjanchi, M. Arvand, Efficient removal of anionic surfactant using partial template-containing MCM-41, Desalination, 284 (2012) 142–149.
[9] M. Hosseinnia, A. Hashtroudiand M.S. Pazouki, M. Banifatemi, Removal of surfactants from wastewater by rice husk, Iran J. Chem. Eng., 3 (2006) 3–9.
[10] M.G. Ivanets, T.A. Savitskaya, T.N. Nevar, D.D. Grinshpan, Adsorption of sodium dodecylsulfate on modified carbon adsorbents, Russ. J. Phys. Chem. A., 86 (2012) 1710–1715.
[11] P. Das Purakayastha, A. Pal, M. Bandyopadhyay, Sorption kinetics of anionic surfactant on to waste tire rubber granules, Sep. Purif. Technol., 46 (2005) 129–135.
[12] H. Xia, X. Zhao, X. Zhao, P. Yao, H. Zhang, Adsorption of sodium dodecyl sulfate onto precipitate in treatment of vat dark blue BO by dissolved air flotation, Environ. Technol. (UK), 39 (2018) 1908–1913.
[13] A.O. Adekanmbi, I.M. Usinola, Biodegradation of sodium dodecyl sulphate (SDS) by two bacteria isolated from wastewater generated by a detergent-manufacturing plant in Nigeria, Jordan J. Biol. Sci., 10 (2017) 251–255.
[14] P.S. Ambily, M.S. Jisha, Biodegradation of anionic surfactant, sodium dodecyl sulphate by *pseudomonas aeruginosa* MTCC 10311, J. Environ. Biol., 33 (2012) 717–720.
[15] C. Korzenowski, M.B.O. Martins, A.M. Bernardes, J.Z. Ferreira, E.C.N.F. Duarteand M.N. De Pinho, Removal of anionic surfactants by nanofiltration, Desal. Water Treat., 44 (2012) 269–275.
[16] I. Kowalska, M. Kabsch-Korbutowicz, K. Majewska-Nowak, T. Winnicki, Separation of anionic surfactants on ultrafiltration membranes, Desalination, 162 (2004) 33–40.
[17] K. Ikehata, M.G. El-Din, Degradation of recalcitrant surfactants in wastewater by ozonation and advanced oxidation processes: A review, Ozone Sci. Eng., 26 (2004) 327–343.
[18] M. Sanchez, M.J. Rivero, I. Ortiz, Kinetics of dodecylbenzenesulphonate mineralisation by TiO_2 photocatalysis, Appl. Catal. B Environ., 101 (2011) 515–521.
[19] T.N. Chikwe, R.E. Ekpo, I. Okoye, Competitive adsorption of organic solvents using modified and unmodified calcium bentonite clay mineral, Chem. Int., 4 (2018) 230–239.
[20] M. Fazal-ur-Rehman, Methodological trends in preparation of activated carbon from local sources and their impacts on production-a review, Chem. Int., 4 (2018) 109–119.
[21] A. Abhishek, N. Saranya, P. Chandi, N. Selvaraju, Studies on the remediation of chromium (VI) from simulated wastewater using novel biomass of *Pinus kesiya* cone, Desal. Water Treat., 114 (2018) 192–204.
[22] E. Nakkeeran, N. Saranya, M.S. Giri Nandagopal, A. Santhiagu, N. Selvaraju, Hexavalent chromium removal from aqueous solutions by a novel powder prepared from *Colocasia esculenta* leaves, Int. J. Phytoremediation 18 (2016) 812–821.
[23] S. Rangabhashiyam, N. Selvaraju, Adsorptive remediation of hexavalent chromium from synthetic wastewater by a natural and $ZnCl_2$ activated *Sterculia guttata* shell, J. Mol. Liq., 207 (2015) 39–49.
[24] E. Suganya, S. Rangabhashiyam, A.V. Lity, N. Selvaraju, Removal of hexavalent chromium from aqueous solution by a novel biosorbent *Caryota urens* seeds: equilibrium and kinetic studies, Desal. Water Treat., 57 (2016) 23940–23950.
[25] S. Rangabhashiyam, E. Suganya, N. Selvaraju, Packed bed column investigation on hexavalent chromium adsorption using activated carbon prepared from *Swietenia Mahogani* fruit shells, Desal. Water Treat., 57 (2016) 13048–13055.
[26] N.E. Ibisi, C.A. Asoluka, Use of agro-waste (*Musa paradisiaca peels*) as a sustainable biosorbent for toxic metal ions removal from contaminated water, Chem. Int., 4 (2018) 52–59.
[27] N. Saranya, A. Ajmani, V. Sivasubramanian, N. Selvaraju, Hexavalent Chromium removal from simulated and real effluents using *Artocarpus heterophyllus* peel biosorbent - Batch and continuous studies, J. Mol. Liq., 265 (2018) 779–790.
[28] S. Rangabhashiyam, E. Suganya, A.V. Lity, N. Selvaraju, Equilibrium and kinetics studies of hexavalent chromium biosorption on a novel green macroalgae *Enteromorpha sp.*, Res. Chem. Intermed., 42 (2016) 1275–1294.
[29] P.S. Bhandari, P.R. Gogate, Kinetic and thermodynamic study of adsorptive removal of sodium dodecyl benzene sulfonate using adsorbent based on thermo-chemical activation of coconut shell, J. Mol. Liq., 252 (2018) 495–505.
[30] A. Adak, A. Pal, M. Bandyopadhyay, Spectrophotometric determination of anionic surfactants in wastewater using acridine orange, Indian J. Chem. Technol., 12 (2005) 145–148.
[31] X. Wang, D. Li, W. Li, J. Peng, H. Xia, L. Zhang, S. Guo, G. Chen, Optimization of mesoporous activated carbon from coconut shells by chemical activation with phosphoric acid, BioResources, 8 (2013) 6184–6195.
[32] P.C. Pavan, E.L. Crepaldi, J.B. Valim, Sorption of anionic surfactants on layered double hydroxides, J. Colloid Interface Sci., 229 (2000) 346–352.
[33] S.R. Taffarel, J. Rubio, Adsorption of sodium dodecyl benzene sulfonate from aqueous solution using a modified natural zeolite with CTAB, Miner. Eng., 23 (2010) 771–779.
[34] C. Moreno-Castilla, Adsorption of organic molecules from aqueous solutions on carbon materials, Carbon, 42 (2004) 83–94.
[35] Y. Zhao, P. Lu, C. Li, X. Fan, Q. Wen, Q. Zhan, X. Shu, T. Xu, G. Zeng, Adsorption mechanism of sodium dodecyl benzene sulfonate on carbon blacks by adsorption isotherm and zeta potential determinations, Environ. Technol., 34 (2013) 201–207.

[36] Y. Ihara, Adsorption of anionic surfactants and related compounds from aqueous solution onto activated carbon and synthetic adsorbent, J. Appl. Polym. Sci., 44 (1992) 1837–1840.
[37] M. Sekar, V. Sakthi, S. Rengaraj, Kinetics and equilibrium adsorption study of lead(II) onto activated carbon prepared from coconut shell, J. Colloid Interface Sci., 279 (2004) 307–313.
[38] V.S. Mane, P.V.V Babu, Studies on the adsorption of Brilliant Green dye from aqueous solution onto low-cost NaOH treated saw dust, Desalination, 273 (2011) 321–329.
[39] R. Ahmad, R. Kumar, Adsorptive removal of congo red dye from aqueous solution using bael shell carbon, Appl. Surf. Sci., 257 (2010) 1628–1633.
[40] N. Barka, M. Abdennouri, M. El Makhfoukand S. Qourzal, Biosorption characteristics of cadmium and lead onto eco-friendly dried cactus (*Opuntia ficus indica*) cladodes, J. Environ. Chem. Eng., 1 (2013) 144–149.
[41] M.H. Kalavathy, T. Karthikeyan, S. Rajgopal, L.R. Miranda, Kinetic and isotherm studies of Cu(II) adsorption onto H_3PO_4-activated rubber wood sawdust, J. Colloid Interface Sci., 292 (2005) 354–362.
[42] S.N. Jain, P.R. Gogate, NaOH-treated dead leaves of *Ficus racemosa* as an efficient biosorbent for Acid Blue 25 removal, Int. J. Environ. Sci. Technol., 14 (2017) 531–542.
[43] S. Rangabhashiyam, N. Selvaraju, Evaluation of the biosorption potential of a novel *Caryota urens* inflorescence waste biomass for the removal of hexavalent chromium from aqueous solutions, J. Taiwan Inst. Chem. Eng., 47 (2015) 59–70.
[44] E. Nakkeeran, S. Rangabhashiyam, M.S. Giri Nandagopal, N. Selvaraju, Removal of Cr(VI) from aqueous solution using *Strychnos nux-vomica* shell as an adsorbent, Desal. Water Treat., 57 (2016) 23951–23964.
[45] J.S. Zogorski, S.D. Faustand J.H. Haas, The kinetics of adsorption of phenols by granular activated carbon, J. Colloid Interface Sci., 55 (1976) 329–341.
[46] S. Lagergren, About the theory of so-called adsorption of soluble substance, K. Sven. Vetenskapsakademiens Handl., 24 (1898) 1–39.
[47] Y.S. Ho, Citation review of Lagergren kinetic rate equation on adsorption reactions, Scientometrics, 59 (2004) 171–177.
[48] Y.S. Ho, G. McKay, A comparison of chemisorption kinetic models applied to pollutant removal on various sorbents, Trans I ChemE., 76 (1998) 332–340.
[49] J.C.Y. Ng, W.H. Cheung, G. McKay, Equilibrium studies of the sorption of Cu(II) ions onto chitosan, J. Colloid Interface Sci., 255 (2002) 64–74.
[50] S. Karaca, A. Gürses, M. Ejder, M. Açikyildiz, Kinetic modeling of liquid-phase adsorption of phosphate on dolomite, J. Colloid Interface Sci., 277 (2004) 257–263.
[51] W.J. Weber, J.C. Morris, Kinetics of adsorption on carbon from solution, J. Sanit. Eng. Div., 89 (1963) 31–60.
[52] I.A.W. Tan, A.L. Ahmad, B.H. Hameed, Adsorption isotherms, kinetics, thermodynamics and desorption studies of 2,4,6-trichlorophenol on oil palm empty fruit bunch-based activated carbon, J. Hazard. Mater., 164 (2009) 473–482.
[53] A.C.A. de Lima, R.F. Nascimento, F.F. de Sousa, J.M. Filho, A.C. Oliveira, Modified coconut shell fibers: A green and economical sorbent for the removal of anions from aqueous solutions, Chem. Eng. J., 185–186 (2012) 274–284.
[54] K.K. Beltrame, A.L. Cazetta, P.S.C. de Souza, L. Spessato, T.L. Silva, V.C. Almeida, Adsorption of caffeine on mesoporous activated carbon fibers prepared from pineapple plant leaves, Ecotoxicol. Environ. Saf., 147 (2018) 64–71.
[55] J. Ma, M. Yang, F. Yu, J. Zheng, Water-enhanced removal of ciprofloxacin from water by porous graphene hydrogel, Sci. Rep., 5 (2015) 13578.
[56] R. Pandey, N.G. Ansari, R.L. Prasad, R.C. Murthy, Pb (II) removal from aqueous solution by *Cucumissativus* (Cucumber) peel : kinetic, equilibrium and thermodynamic study, Am. J. Environ. Prot., 2 (2014) 51–58.
[57] S. Nethaji, A. Sivasamyand A.B. Mandal, Adsorption isotherms, kinetics and mechanism for the adsorption of cationic and anionic dyes onto carbonaceous particles prepared from *Juglans regia* shell biomass, Int. J. Environ. Sci. Technol., 10 (2012) 231–242.
[58] L. Yu, Y.M. Luo, The adsorption mechanism of anionic and cationic dyes by Jerusalem artichoke stalk-based mesoporous activated carbon, J. Environ. Chem. Eng., 2 (2014) 220–229.
[59] A. Mittal, J. Mittal, A. Malviya, V.K. Gupta, Adsorptive removal of hazardous anionic dye "Congo red" from wastewater using waste materials and recovery by desorption, J. Colloid Interface Sci., 340 (2009) 16–26.
[60] K.Y. Foo, B.H. Hameed, Insights into the modeling of adsorption isotherm systems, Chem. Eng. J., 156 (2010) 2–10.
[61] I. Langmuir, Adsorption of gases on plane surfaces of glass, mica and platinum, J. Am. Chem. Soc., 40 (1918) 1361–1403.
[62] H.M.F. Freundlich, Over the adsorption solutions, J. Phys. Chem., 57 (1906) 385–470.
[63] L. Huang, Y. Sun, T. Yang, L. Li, Adsorption behavior of Ni (II) on lotus stalks derived active carbon by phosphoric acid activation, Desalination, 268 (2011) 12–19.
[64] M. Temkin, V. Pyzev, Kinetics of ammonia synthesis on promoted iron catalyst, Acta Physicochim USSR, 12 (1940) 217–225.
[65] A. Dada, A. Olalekan, A. Olatunyaand O. Dada, Langmuir, Freundlich, Temkin and Dubinin – Radushkevich isotherms studies of equilibrium sorption of Zn^{2+} unto phosphoric acid modified rice husk, IOSR J. Appl. Chem., 3 (2012) 38–45.
[66] S. Gupta, A. Pal, P.K. Ghosh, M. Bandyopadhyay, Performance of waste activated carbon as a low-cost adsorbent for the removal of anionic surfactant from aquatic environment, J. Environ. Sci. Health. A. Tox. Hazard. Subst. Environ. Eng., 38 (2003) 381–397.
[67] S.N. Jain, P.R. Gogate, Efficient removal of Acid Green 25 dye from wastewater using activated Prunus Dulcis as biosorbent: Batch and column studies, J. Environ. Manage., 210 (2018) 226–238.
[68] I.A.W. Tan, B.H. Hameed, Adsorption isotherms, kinetics, thermodynamics and desorption studies of basic dye on activated carbon derived from oil palm empty fruit bunch, J. Appl. Sci., 10 (2010) 2565–2571.
[69] A. Gurses, M. Yalcin, M. Sozbilir, C. Dogar, The investigation of adsorption thermodynamics and mechanism of a cationic surfactant, CTAB, onto powdered active carbon, Fuel Process. Technol., 81 (2003) 57–66.
[70] K. Namasivayam, C. Muniasamy, N. Gayatri, K. Rani, M. Rangnathan, Removal of dyes from aqueous solutions by cellulosic waste orange peel, Bioresource Technol., 57 (1996) 37–63.
[71] G. Crini, Recent developments in polysaccharide-based materials used as adsorbents in wastewater treatment, Prog. Polym. Sci., 30 (2005) 38–70.
[72] P. Das Purakayastha, A. Pal, M. Bandyopadhyay, Adsorbent selection for anionic surfactant removal from water, Indian J. Chem. Technol., 12 (2005) 281–284.
[73] T.K. Sen, M.T. Thi, S. Afroze, C. Phan, M. Ang, Removal of anionic surfactant sodium dodecyl sulphate from aqueous solution by adsorption onto pine cone biomass of *Pinus Radiate*: equilibrium, thermodynamic, kinetics, mechanism and process design Removal of anionics, Desal. Water Treat., 45 (2012) 263–275.
[74] G. Moussavi, S. Shekoohiyan, S. Mojab, Adsorption capacity of NH_4Cl-induced activated carbon for removing sodium dodecyl sulfate from water, Desal. Water Treat., 57 (2016) 11283–11290.